

1 **Projected increases in wildfires may challenge regulatory curtailment of PM<sub>2.5</sub> over the**  
2 **eastern US by 2050**

3

4 Chandan Sarangi<sup>1,2\*</sup>, Yun Qian<sup>2\*</sup>, L. Ruby Leung<sup>2</sup>, Yang Zhang<sup>3</sup>, Yufei Zou<sup>4,2</sup>, Yuhang  
5 Wang<sup>4</sup>

6

7 <sup>1</sup> Indian Institute of Technology Madras, Chennai, India

8 <sup>2</sup> Pacific Northwest National Laboratory, Richland, WA, USA

9 <sup>3</sup> Department of Civil and Environmental Engineering, Northeastern University, Boston, MA

10 <sup>4</sup> School of Earth and Atmospheric Sciences, Georgia Institute of Technology, Atlanta, GA,  
11 USA.

12

13

14 \*Corresponding Authors:

15 [chandansarangi@iitm.ac.in](mailto:chandansarangi@iitm.ac.in)

16 [yun.qian@pnnl.gov](mailto:yun.qian@pnnl.gov)

17

18

19

20

21 **Abstract**

22 Anthropogenic contribution to the overall fine particulate matter (PM<sub>2.5</sub>) concentrations has  
23 been declining sharply in North America. In contrast, a steep rise in wildfire-induced air  
24 pollution events with recent warming is evident in the region. Here, based on coupled fire-  
25 climate-ecosystem model simulations, summertime wildfire-induced PM<sub>2.5</sub> concentrations are  
26 projected to nearly double in North America by the mid-21st century compared to the  
27 present. More strikingly, the projected enhancement in fire-induced PM<sub>2.5</sub> (~ 1-2 µg/m<sup>3</sup>) and  
28 its contribution (~15-20%) to the total PM<sub>2.5</sub> are distinctively significant in the eastern US.  
29 This can be attributed to downwind transport of smoke from future enhancement of wildfires  
30 in North America to the eastern US and associated positive climatic feedback on PM<sub>2.5</sub> i.e.  
31 perturbations in circulation, atmospheric stability and precipitation. Therefore, the anticipated  
32 reductions in PM<sub>2.5</sub> from regulatory controls on anthropogenic emissions could be  
33 significantly compromised in the future in the densely populated eastern US.

34 **Key points:**

- 35 1) Wildfire-PM<sub>2.5</sub> associations studied based on unprecedented two-way coupled fire-  
36 climate-ecosystem model simulations
- 37 2) A steep rise in wildfire-induced air pollution events with recent warming is evident in  
38 the region
- 39 3) The transported smoke from enhanced wildfires in North America can severely affect  
40 air quality over Eastern US

41

42 **Keywords:** wildfire emissions, climate change, air quality, smoke transport, wildfire-climate-  
43 ecosystem interactions

## 44 **1. Introduction**

45 Wildfires are widespread burning events in forests, shrub lands, and grazing lands. In  
46 North America (mainly Canada and the US), particulate matter emissions from wildfires are a  
47 significant source of regional air pollution (Shi et al., 2019; McClure and Jaffe, 2018; Van  
48 Der Werf et al., 2010; Jaffe et al., 2008). Since the 1980s, the number of large wildfires and  
49 the length of wildfire season have been increasing, and the trends are projected to continue in  
50 the future over the western US, Alaska and Canada (Kitzberger et al., 2017; Kirchmeier-  
51 Young et al., 2017; Abatzoglou and Williams, 2016; Partain et al., 2016; Jolly et al., 2015;  
52 Westerling et al., 2006; Gillett et al., 2004). Accordingly, particulate emissions from wildfires  
53 are also anticipated to increase in North America in the 21st century (Knorr et al., 2017; Liu  
54 et al., 2016; Val Martin et al., 2015). Human exposure to high concentrations of wildfire-  
55 emitted airborne particulate matter of diameter  $\leq 2.5 \mu\text{m}$  (PM<sub>2.5</sub>) is known to have substantial  
56 adverse effects on pulmonary and cardiovascular functioning (Anjali et al., 2019; Black et al.,  
57 2017), which contribute significantly to global and regional all-cause mortality (Zhang et al.,  
58 2020; Hong et al., 2019; Yang et al., 2019; Ford et al., 2018; Johnston. et al., 2012).  
59 Therefore, a better understanding of the future changes in wildfire-induced PM<sub>2.5</sub> and its  
60 contribution to the total surface PM<sub>2.5</sub> is essential.

61 In the last two decades, ambient air quality in the US has substantially improved due  
62 to a decline in PM<sub>2.5</sub> by ~ 40 % (US EPA, 2018). The decrease in PM<sub>2.5</sub> is primarily due to  
63 curtailment of anthropogenic emissions resulting from US-based efforts to meet regulations  
64 such as the Clean Air Act (US EPA, 2009), Cross-State Air Pollution Rule, Regional Haze  
65 Rule, and the motor vehicles emissions standards. Consequently, air quality over the  
66 contiguous US (CONUS) and Canada has improved steadily such that it is predicted to  
67 achieve the targeted National Ambient Air Quality Standards in the future (Nolte et al.,

68 2018). Under this promising scenario, the influence of wildfire-emissions on the total PM<sub>2.5</sub>  
69 becomes even more crucial. Depending on the competition between climate-induced increase  
70 in wildfires and the regulatory control on anthropogenic emissions, future enhancement in  
71 wildfire-induced PM<sub>2.5</sub> may compromise the reduction in anthropogenic PM<sub>2.5</sub> concentrations  
72 in certain regions. In agreement, recent studies have highlighted the potential for future  
73 enhancement in wildfire-induced pollution to diminish the reducing trend in PM<sub>2.5</sub>, primarily  
74 over the western US (O'Dell et al., 2019; Ford et al., 2018; Val Martin et al., 2015; Yue et al.,  
75 2013).

76         While the fractional wildfire burnt area and fire intensities are the greatest over the  
77 western US and Canadian regions within North America, anthropogenic emissions dominate  
78 the ambient PM<sub>2.5</sub> concentration over the eastern US. The inherent geographical separation  
79 between the regions with large wildfire emissions and anthropogenic emissions leads to a  
80 pertinent question: will future enhancement in wildfires over the western US and Canada  
81 have significant effects on PM<sub>2.5</sub> over the eastern US? Addressing this question is crucial  
82 because the declining trend in PM<sub>2.5</sub> over the eastern US is the major contributor to the  
83 observed 40% decrease in PM<sub>2.5</sub> over the US in the last two decades (US EPA, 2018).  
84 Eastward advection of wildfire smoke from Canada and the western US has been found to  
85 severely hamper the surface air quality of the central and eastern US under the influence of  
86 the prevailing westerlies during the summer months (Brey et al., 2018; Wu et al., 2018;  
87 Gunsch et al., 2018; Kaulfus et al., 2017; Dempsey, 2013). The transported wildfire smoke  
88 can influence the meteorology and climate via the radiative impact of carbonaceous  
89 emissions, changes in land albedo and cloud system perturbations (Ward et al., 2012; Liu et  
90 al., 2014). These fire-weather interactions can have positive feedback on the locally-emitted  
91 PM<sub>2.5</sub> in the eastern US by surface cooling and boundary layer suppression(Guan et al.,  
92 2020). At the same time, fire-triggered ecosystem changes can induce negative feedback on

93 PM<sub>2.5</sub> by reducing the future wildfires over North America (Zou et al., 2020). Thus, two-  
94 way interactions between fires and climate that are important for predicting future changes in  
95 wildfire locations, intensities, and durations (Harris et al., 2016) as well as associated  
96 particulate emissions is essential. However, past studies have mostly employed simple  
97 statistical models based on statistical regressions of present-day fire burnt area on the  
98 meteorological fields (Liu et al., 2016; Spracklen et al., 2009; Yue et al., 2013; Val Martin et  
99 al., 2015), and more recently, one-way coupled modelling (Ford et al., 2018; O’Dell et al.,  
100 2019).

101 Here, based on new two-way coupled fire-climate-ecosystem simulations, we  
102 demonstrate the significance of wildfire-induced contributions to ambient PM<sub>2.5</sub> over the  
103 eastern US due to enhanced wildfire smoke transportation and smoke-induced changes in  
104 weather in eastern US. This enhancement in wildfire-induced PM<sub>2.5</sub> may potentially challenge  
105 the targeted policy-driven reduction of PM<sub>2.5</sub> in the eastern US. Next, our model setup,  
106 experiments and methodology are explained in Section 2, followed by results and discussion  
107 in Section 3. The study is summarized in Section 4.

## 108 **2. Materials and Methods**

### 109 **2.1. RESFire-CESM Model description**

110 We employ the open-source REgion-Specific ecosystem feedback fire (RESFire)  
111 model coupled with the Community Land Model version 4.5 and the Community  
112 Atmosphere Model version 5 (CAM5) of the Community Earth System Model (CESM)  
113 version 1 (Zou et al., 2019; Neale et al., 2013) to perform two-way coupled simulations.  
114 RESFire provides state-of-the-art capabilities to simulate the complex fire-climate-ecosystem  
115 interactions globally for fires occurring over wildland, cropland, and peatland. Although  
116 wildfires dominate in the North American region, RESFire simulates both wildfires and

117 prescribed fires. Moreover, this integrated setup includes climatic feedback from fire-induced  
118 aerosol direct and indirect radiative effects and associated weather changes. It also includes  
119 feedback from fire-induced vegetation distribution changes and associated biophysical  
120 processes such as evapotranspiration and surface albedo. Sofiev et al. (2012) described the  
121 fire plume rise parameterization. Other features in CLM4.5 and CAM5, such as the  
122 photosynthesis scheme (Sun et al., 2012), the MAM3 aerosol module (Liu et al., 2012), and  
123 the cloud macrophysics scheme (Park et al., 2014), allow for more comprehensive  
124 assessments of the climate effects of fires through their interactions with vegetation and  
125 clouds. Fire-ecosystem interactions are modelled by simulating fire-induced vegetation  
126 mortality and regrowth (and associated land cover change) in RESFire. This approach has  
127 been introduced in Zou et al. (2019) and the simulated ecological and climatic effects of  
128 wildfires have been evaluated in two sets of sensitivity experiments in Zou et al. (2020).  
129 Although fire-climate-ecosystem interactions are considered in this study, our focus is on the  
130 fire-induced changes in PM<sub>2.5</sub> over Canada and the US, so the two vegetation-focused  
131 sensitivity experiments reported in Zou et al. (2020) are not included in this paper. Please  
132 refer to Zou et al. (2019) and Zou et al. (2020) for more details about the simulation of fire-  
133 ecosystem interactions.

## 134 **2.2 Numerical Experiment and Methodology**

135 We designed two sets of simulations for the present day and future scenarios to  
136 quantify the impacts of fire-climate-ecosystem interactions (Table 1). The spatial resolution is  
137 0.9° (lat) × 1.25° (lon) with a time step of 30 min. In each set of simulations, we conducted a  
138 default all emission included control run (X<sub>ALL</sub>, where x=2000 or 2050 indicates the present  
139 day or future, respectively) and a sensitivity run with no wildfire emissions to the atmosphere  
140 (X<sub>WEF</sub>, where X is the same as for the control runs). The ALL runs are designed to simulate  
141 fully interactive fire disturbances such as fire emissions with plume rise and fire induced land

142 cover changes of the present day (representative of the 2000s, 2000<sub>ALL</sub>) and a moderate future  
 143 emission scenario (representative of the 2050s, 2050<sub>ALL</sub>) via the RCP4.5. The only difference  
 144 between the ALL and WEF scenario is that wildfire emissions are absent in the WEF  
 145 scenario. Specifically, in the WEF runs, the online simulated fire emissions are not passed to  
 146 the CAM5 atmosphere model so that the difference between the ALL and WEF runs can be  
 147 used to isolate the atmospheric impacts of fire-climate interactions.

148 Table 1: Summary of the sensitivity simulations performed

Scenario	Present-day		Future	
Experiment Name	2000 <sub>ALL</sub>	2000 <sub>WEF</sub>	2050 <sub>ALL</sub>	2050 <sub>WEF</sub>
Simulation years	2001-2010	2001-2010	2051-2060	2051-2060
Atmosphere	CAM5	CAM5	CAM5	CAM5
Land	CLM4.5	CLM4.5	CLM4.5	CLM4.5
Ocean	Climatology	Climatology	RCP4.5	RCP4.5
Sea ice	Climatology	Climatology	RCP4.5	RCP4.5
Non-fire emissions	ACCMIP	ACCMIP	RCP4.5	RCP4.5
Fire emissions	Online fire aerosols with plume rise	—	Online fire aerosols with plume rise	—
Land cover	Fire disturbances on present-day condition	Fire disturbances on present-day condition	Fire disturbances on RCP4.5 condition	Fire disturbances on RCP4.5 condition

149  
 150 For the present-day experiments, we used the spun-up states from Zou et al. (2019) as  
 151 initial conditions for both meteorological and chemical variables. Sea surface temperature  
 152 (SST) for the present day was obtained from the Met Office Hadley Centre (HadISST).  
 153 Present-day non-fire emissions from anthropogenic and other sources were based on  
 154 ACCMIP (Lamarque et al., 2010) for the year 2000. We replaced the prescribed GFED2 fire  
 155 emissions (van der Werf et al., 2006) in the default setting of CESM with the online-coupled  
 156 fire emissions generated by the RESFire model. Zou et al. (2019) provided more details of  
 157 the physics parameterizations and modeling experiment settings used in these simulations.

158 Land use and land cover data for 2000 and 2050 from the Land-Use History A product (Hurtt  
159 et al., 2006) are used to initialize the 2000<sub>ALL</sub>/2000<sub>WEF</sub> and 2050<sub>ALL</sub>/2050<sub>WEF</sub> simulations,  
160 respectively. Following the above setup, the future scenario 2050<sub>ALL</sub> experiment accounts for  
161 both fuel load changes associated with the projected land use and land cover change  
162 (LULCC) in the 2050s and fire weather changes driven by the SST and sea ice forcing from a  
163 coupled CESM simulation following the greenhouse gas (GHG) forcing of the RCP4.5  
164 scenario. The global mean GHG mixing ratios in the CAM5 atmosphere model were fixed at  
165 the year 2000 levels in all the present-day experiments and they were replaced by those of the  
166 RCP4.5 scenario with the well-mixed assumption and monthly variations. However, the  
167 future population and socioeconomic conditions were identical to those of the present day so  
168 there was no explicit impact of human-induced mitigation/enhancement effects on wildfires  
169 in the future projection in all the future experiments. Future human impacts were considered  
170 implicitly in LULCC-induced fuel load changes in the RCP4.5 scenario.

171 The net projected changes by 2050s in emissions, meteorology and air quality during  
172 summer (JJA: June, July, August) months are estimated by comparing decadal-mean values  
173 simulated by 2000<sub>ALL</sub> with 2050<sub>ALL</sub>. Wildfire-induced enhancement in PM<sub>2.5</sub> concentration in  
174 the present day and mid-21<sup>st</sup> century is estimated by comparing 2000<sub>ALL</sub> with 2000<sub>WEF</sub> and  
175 2050<sub>ALL</sub> with 2050<sub>WEF</sub>, respectively. Further, the projected increase in wildfire-induced  
176 PM<sub>2.5</sub> in the future is calculated by comparing the simulated wildfire effect of the 2050s  
177 (2050<sub>ALL</sub>-2050<sub>WEF</sub>) with that of the 2000s (2000<sub>ALL</sub>-2000<sub>WEF</sub>). With large spatiotemporal  
178 variability, the projected changes in transported fire-emissions from the western US and  
179 Canada to the eastern US by the 2050s and the corresponding impacts are summarized using  
180 probability distribution functions. The latter provide information not only for the mean but  
181 also variability and extreme values to quantify the simulated changes for the three subregions.

182



### 183 **3. Results and Discussion**

#### 184 **3.1 Model Evaluation**

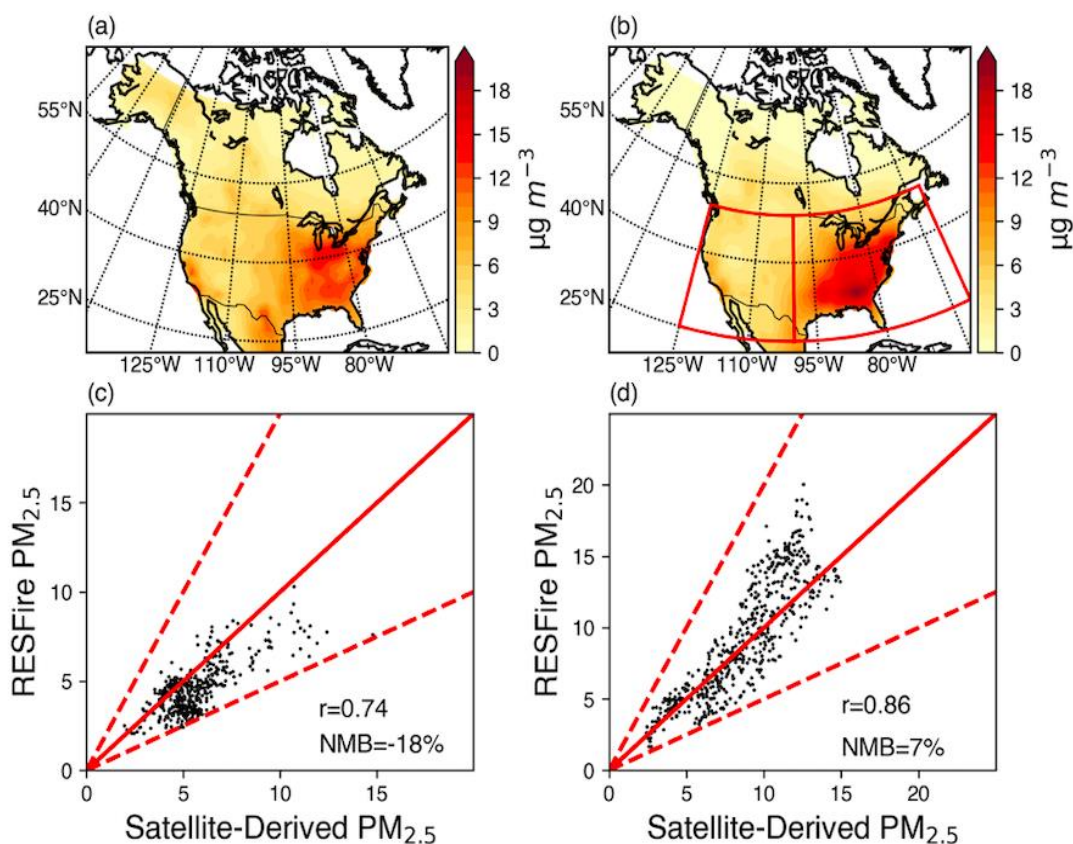
185 Zou et al. (2019) performed comprehensive evaluation of the RESFire simulated  
186 wildfire burnt area distribution, associated carbon emissions and terrestrial carbon balance to  
187 demonstrate reasonable model skill. Zou et al. (2020) compares global fire simulations by  
188 CESM-RESFire with modeling results reported in the literature to show better agreement  
189 with the GFED4.1s benchmark data and predicts more prominent changes in the future than  
190 those predicted by Kloster et al. (2010, 2012). These differences might come from differences  
191 in the climate sensitivities of the fire models and scenarios and other input data used to make  
192 future projections.

193 Here, we evaluate the simulated surface PM<sub>2.5</sub> against satellite-estimates (Figure 1)  
194 over North America. The PM<sub>2.5</sub> concentration is calculated as the sum of sulfate, nitrate, fine  
195 sea salt (first 2 size bins), fine dust (first size bin), black carbon (BC), and organic aerosol  
196 (OC) at the surface-level of model. OC is the sum of primary organic matter (POM) and  
197 secondary organic aerosol (SOA), and SOA is the sum of secondary species formed from  
198 toluene, monoterpenes, isoprene, benzene, and xylene. Figure 1 compares the observed and  
199 simulated mean annual PM<sub>2.5</sub> averaged over 2001-2010. The 10-year average satellite AOD-  
200 derived annual mean surface PM<sub>2.5</sub> concentrations (Van Donkelaar et al., 2018) are regridded  
201 to the model grid (Figure 1A) and then compared with the RESFire simulations in the  
202 2000<sub>ALL</sub> present-day run (Figure 1B). The spatial distribution of annual surface PM<sub>2.5</sub> is  
203 reasonably well simulated but also have some biases. To quantify the biases, we also  
204 estimated the correlation coefficient as well as normalized mean biases (NMB) of the  
205 simulated values compared against the satellite retrieved values over two subregions.  
206 Quantitatively, the NMB values over the western US (WUS) and eastern US (EUS) are 18%  
207 and 7%, respectively (Figure 1C-D). In addition, the spatial variability of the 2001-2010

208 averaged annual AOD distribution (Supplementary Figure 1) is also well represented in our  
209 simulation, although the model underestimates high AOD values. Similar spatial variability  
210 and biases in AOD and PM<sub>2.5</sub> were also found when a comparison was performed for only  
211 summer months (June through August; JJA). The simulated PM<sub>2.5</sub> has also been evaluated  
212 against the ground-based Interagency Monitoring of Protected Visual Environments  
213 (IMPROVE) data, showing similar spatial pattern and biases (10-25%) (Supplementary  
214 Figure 2). The biases are smaller over Eastern US and Southwestern US region. The  
215 simulated PM<sub>2.5</sub> values over California matches quite well with the observed annual mean  
216 values. However, the biases over Northwestern US region are ~30-40%, a portion of which  
217 could be attributed to possible biases in model's meteorology in northwestern US region.  
218 Nonetheless, both satellite and in situ evaluation indicate that our simulation biases are  
219 largely within the uncertainty range among the various satellite and ground-based datasets,  
220 which have normalized mean biases ranging from -3.3% to 33.3% when benchmarked against  
221 the ground-based IMPROVE data over the contiguous US (Diao et al., 2019; Val Martin et al.  
222 (2015)).

223         Discrepancies between the simulated and observed PM<sub>2.5</sub> values may be attributed to  
224 several potential reasons. First, the satellite-derived data has a non-zero lower bound of PM<sub>2.5</sub>  
225 concentrations, so the ambient background concentrations for relatively cleaner regions such  
226 as the western US may be overestimated (Figure 1C), also the sampling frequency between  
227 these datasets are different. Second, year 2000-based constant non-fire emissions were used  
228 in the RESFire simulation, which may result in overestimation of the PM<sub>2.5</sub> concentrations  
229 from non-fire sources during 2001-2010 when anthropogenic emissions and PM<sub>2.5</sub>  
230 concentrations continue to decrease (US EPA, 2018). This overestimation is prominent in  
231 regions dominated by non-fire sources such as the southeastern US. Third, large uncertainties  
232 in fuel consumption and emission factors preclude an accurate estimation of the primary fire

233 emissions in the model, especially for the eastern US where large fractions of low-intensity  
 234 prescribed fires consume only under-canopy fuels such as litter and duff layers. The fire  
 235 model may fail to capture the subtle distinctions between low-intensity prescribed fires and  
 236 forest fires, so more fuels are consumed and result in higher emissions. Lastly, comparison of  
 237 a coarsely resolved simulation against in-situ observations also contributes to uncertainty.  
 238 Differences in the degree to which fire-climate interactions and other physical processes and  
 239 feedbacks are represented by the models can explain the slight differences in estimating the  
 240 present day mean wildfire-induced change in PM<sub>2.5</sub> over local and downwind regions  
 241 between our simulations and previous studies. Nonetheless, reasonable simulation of the  
 242 spatial distribution of wildfire burnt area, AOD, and near surface particulate concentration  
 243 (mean bias of ~10-20 %) instills confidence about the fidelity of our model setup in  
 244 particulate pollution simulation, which is the focus of this study.



245  
 246

247 Figure 1: Comparison of the 10-year (2001-2010) averaged annual mean surface PM<sub>2.5</sub>  
248 concentration between observations and RESFire simulations. (a) Satellite-derived surface  
249 PM<sub>2.5</sub> concentrations (with dust and sea-salt removed) estimated by Donkelaar et al., 2018  
250 (available at [https://sedac.ciesin.columbia.edu/data/set/sdei-global-annual-gwr-pm2-5-modis-](https://sedac.ciesin.columbia.edu/data/set/sdei-global-annual-gwr-pm2-5-modis-misr-seawifs-aod)  
251 [misr-seawifs-aod](https://sedac.ciesin.columbia.edu/data/set/sdei-global-annual-gwr-pm2-5-modis-misr-seawifs-aod); last access: 5 November, 2021); (b) 2000<sub>ALL</sub> Simulated surface PM<sub>2.5</sub>  
252 concentrations (with dust and sea-salt removed) averaged over 2001-2010; The red boxes  
253 denote the two subregions (EUS and WUS) shown in Fig. 2 in the main text. (c) comparison  
254 of simulated and satellite based gridded surface PM<sub>2.5</sub> concentrations in the WUS subregion;  
255 Number of samples is equal to the number of land grids ~450 (d) same as (c) but in the EUS  
256 subregion. Number of samples is equal to the number of land grids ~375 The red solid and  
257 dashed lines denote the 1:1 ratio line and  $\pm 100\%$  biases, respectively. The correlation  
258 coefficients and NMB values are shown at the lower-right corner of each subplot.

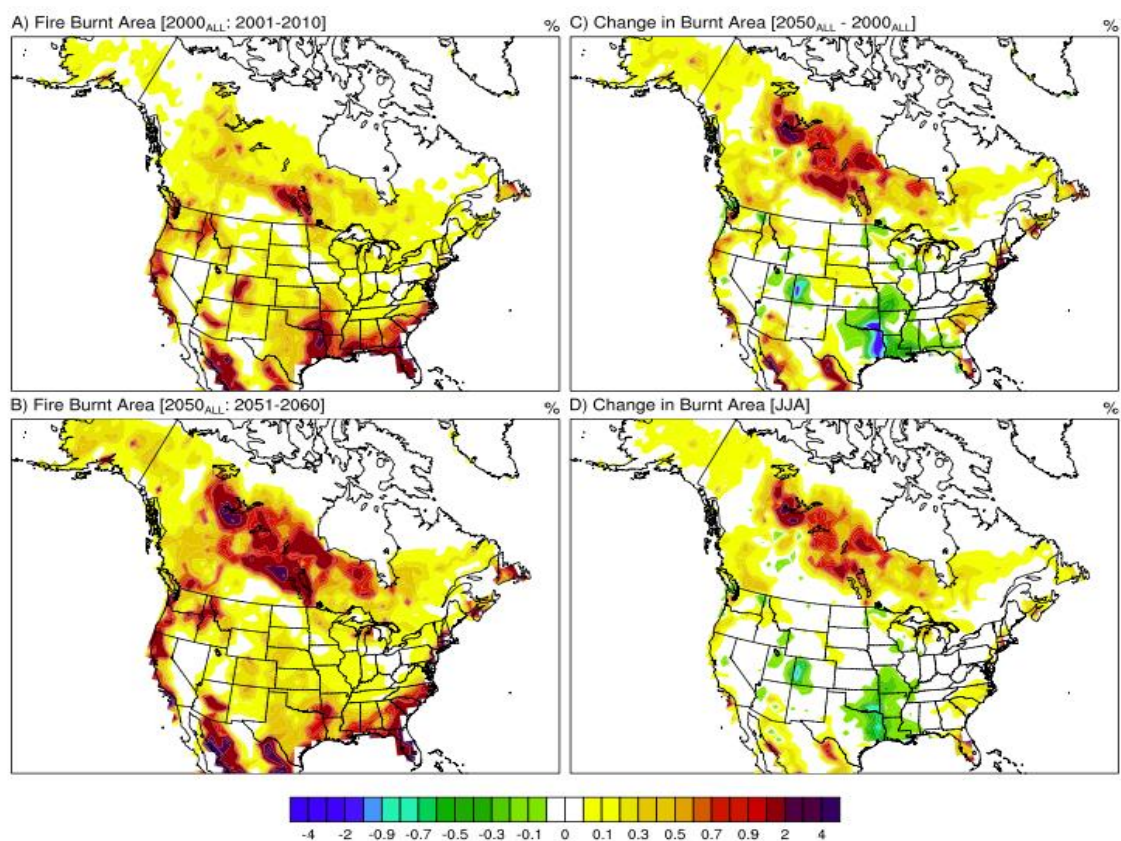
259

### 260 **3.2 Fire-induced changes in burnt area and PM<sub>2.5</sub>**

261 The decadal-mean annual fire burnt area simulated for the present day shows  
262 widespread wildfires over the entire North America (Figure 2A). Specifically, Canada and the  
263 forested areas of the northwestern ( $> 36$  N latitude) and southeastern ( $< 36$  N latitude) US are  
264 most intensely affected by wildfires in the present day. By the mid-21<sup>st</sup> century, a striking  
265 increase of 2-5 times in fire burnt area is projected over Canada, Alaska, the Pacific  
266 Northwest and portions of the western US by the 2050s (Figure 2B). A distinct positive shift  
267 in the probability density function (PDF) of annual fire burnt area is evident in the future,  
268 with the decadal-mean difference statistically significant at the 99% confidence level (Zou et  
269 al., 2020). A small and statistically insignificant change in interannual variability ( $\sim 0.4$  Mha  
270  $\text{yr}^{-1}$ ) of fire burnt areas is also simulated between the present and future. Specifically, our  
271 model predicts more than a doubling of burnt area in boreal regions of Canada in the future,  
272 in line with a previous projection for Canada (Wotton et al., 2017). Future enhancement in  
273 fire burnt area is  $\sim 20$ -50% in most fire grids over the western coast of US, which is higher  
274 than that over the eastern US (Figures 2A and 2C). The increase over the western US is closer  
275 to the lower bound of that derived from statistical model ensemble projections for the western  
276 US in the mid-21<sup>st</sup> century (Yue et al., 2013). The statistics-based projections of future burnt

277 area over North America were likely too high because fire-induced land cover change, fuel  
278 load reduction and factors could induce a negative fire feedback, which was not considered in  
279 previous fire projection studies (Zou et al. 2020).

280 Annual fire burnt area in the southeastern US shows a decline in the future (Figure  
281 2C), as precipitation is projected to increase in that region (discussed later). Note that all  
282 future fire changes between 2050<sub>ALL</sub> and 2000<sub>ALL</sub> are primarily associated with climate  
283 warming in response to the increase in greenhouse gas (GHG) concentrations in the RCP4.5  
284 scenario. No direct impacts of population and socioeconomic changes on wildfires are  
285 included in our simulations, although these factors contribute to changes in GHG emissions  
286 (via the RCP scenario) that influence the climate simulated in 2000<sub>ALL</sub> and 2050<sub>ALL</sub>. As about  
287 80% of the projected fire changes in the future is restricted to the summer season (June  
288 through August; JJA) (Figure 2D), we focus on analysis of the summer-mean wildfire-  
289 induced PM<sub>2.5</sub> and its projected future changes over North America.



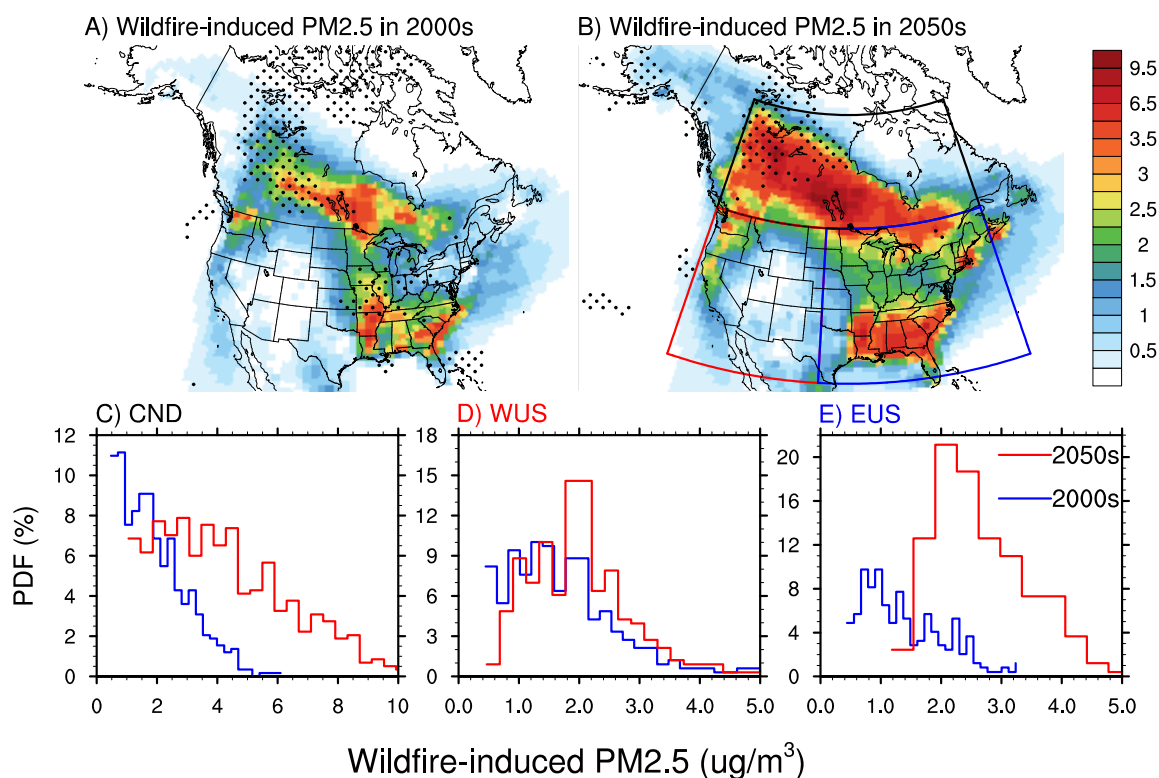
290

291 Figure 2: **Spatial distribution of fire burnt area. A-D**, Spatial distribution of simulated  
292 decadal-mean annual burnt area (as percentage) over North America for present day (A),  
293 mid-21<sup>st</sup> century (B) and the net change between the 2050s and the 2000s (C). **D**, same as  
294 (C), but for wildfire burnt area during summer only (June through August; JJA). The colorbar  
295 illustrate grid fraction of area burnt.

296  
297 The simulated 10-year averaged summer-mean wildfire-induced PM<sub>2.5</sub> values in  
298 2000<sub>ALL</sub> are more than 0.5 µg/m<sup>3</sup> over a large part of North America in the present day, with  
299 noticeably larger values (> 1 µg/m<sup>3</sup>) in Canada and the northwestern, central, and  
300 southeastern US (Figure 3A). Interestingly, the spatial distribution of wildfire-induced  
301 PM<sub>2.5</sub> > 1 µg/m<sup>3</sup> resembles an inverted horse-shoe shape. The inverted horse-shoe shaped  
302 spatial distribution is also consistent with the wildfire-smoke climatology derived from the  
303 satellite-guided operational smoke product of the Hazard Mapping System (HMS) during  
304 2005-2015 (Brey et al., 2018; Kaulfus et al., 2017). By the mid-21<sup>st</sup> century, the spatial extent  
305 of the horse-shoe shape for areas with wildfire-induced PM<sub>2.5</sub> enhancement > 1 µg/m<sup>3</sup>  
306 expands significantly to span most regions of North America, with the most pronounced  
307 enhancement occurring over Canada (Figure 3B). The PDFs of the spatial distribution for the  
308 three regions can be seen in Figure 3C-E. Specifically, wildfire induced PM<sub>2.5</sub> in the 2000s  
309 over Canada, WUS and EUS during summer is ~ 1-3 µg/m<sup>3</sup>, 1-3 µg/m<sup>3</sup> and 0.6-1.2 µg/m<sup>3</sup>,  
310 respectively. Maximum values within the WUS region are found over the Pacific Northwest,  
311 with most areas having wildfire induced PM<sub>2.5</sub> values of ~ 2-3 µg/m<sup>3</sup>. Similarly, the southern  
312 states have relatively high wildfire induced PM<sub>2.5</sub> concentrations of ~ 2-4 µg/m<sup>3</sup> within the  
313 EUS in the present-day simulation.

314 Compared to the 2000s, the wildfire induced JJA-averaged PM<sub>2.5</sub> values are almost  
315 doubled to ~ 3-6 µg/m<sup>3</sup> over Canada in the 2050s (Figure 3B and Figure 3C). Consistently,  
316 the values of wildfire induced PM<sub>2.5</sub> over WUS (mainly coastal) also doubled in 2050s  
317 compared to 2000s, with modal values of ~ 2-2.5 µg/m<sup>3</sup> (Figure 3D). Most interestingly, the  
318 enhancement in wildfire-induced summer-mean PM<sub>2.5</sub> over the northern EUS is also

319 significant by the 2050s (Figures 3B). Largely, the summer-mean wildfire-induced PM<sub>2.5</sub>  
 320 concentration over EUS increases from ~0.8 to ~2 μg/m<sup>3</sup> in the mid-century to values of 1.2-  
 321 3.0 μg/m<sup>3</sup> (Figure 3E). The summer-mean wildfire-induced PM<sub>2.5</sub> is thus projected to double  
 322 in North America by the 2050s compared to the 2000s, with a substantial coverage over the  
 323 EUS. An important finding from these PDFs appears to be that there are fewer grids with < 1  
 324 μg/m<sup>3</sup> wildfire induced PM<sub>2.5</sub>, or alternatively, that more regions are being influenced by  
 325 PM<sub>2.5</sub>, and many areas that were already seeing wildfire impacts are seeing enhanced  
 326 impacts. Such enhancement is found not only at the surface but also in an elevated  
 327 atmospheric layer over EUS between 900 and 700 hPa. This is nonintuitive given the fact that  
 328 the increase in fire-burnt area by mid-century over the EUS is not substantial.



329

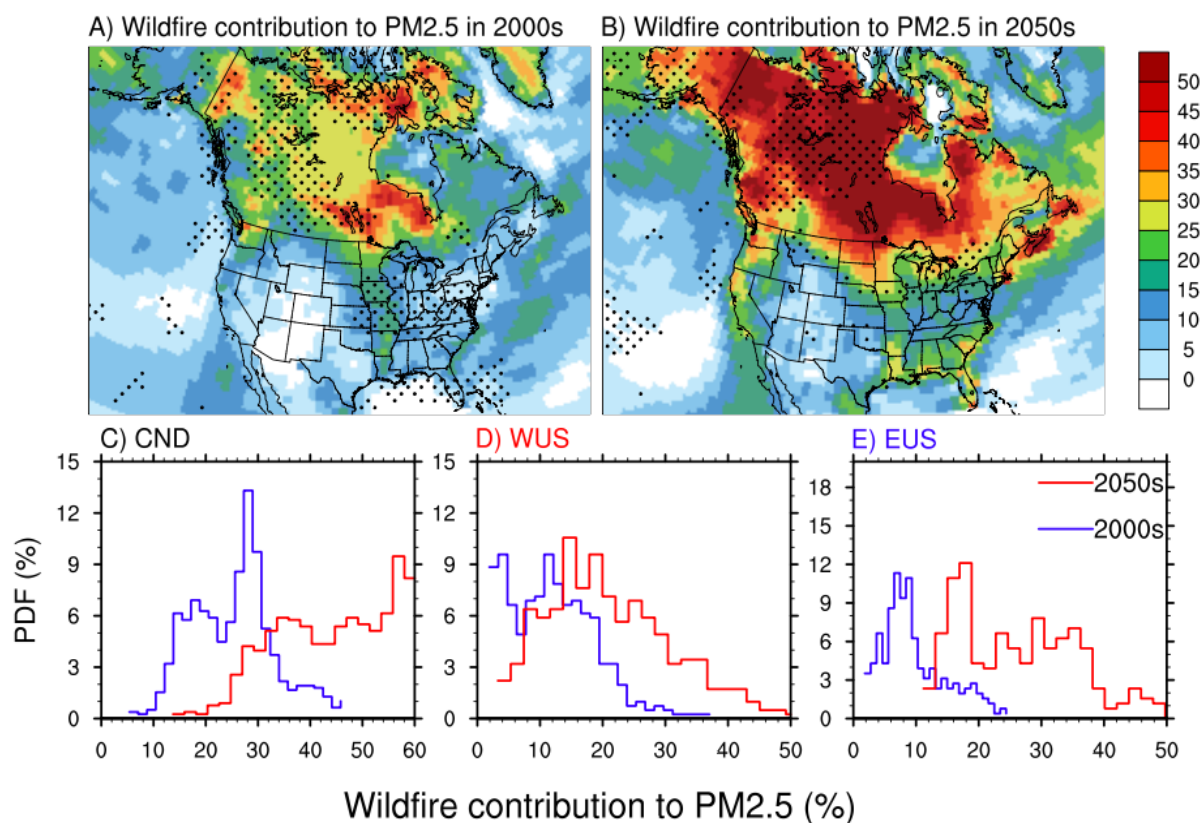
330 **Figure 3: Spatial distribution of PM<sub>2.5</sub> concentrations.** Spatial distribution of decadal-mean  
 331 wildfire-induced enhancement in summer (June through August; JJA) PM<sub>2.5</sub> concentration  
 332 over North America for present day (A, 2000<sub>ALL</sub>-2000<sub>WEF</sub>) and future (B, 2050<sub>ALL</sub>-2050<sub>WEF</sub>).  
 333 The grids with statistical significance of 90% is identified by black dots. C-E, Probability  
 334 density functions (PDFs) of wildfire contribution within the three regions shown in Figure 2B

335 for Canada (CND: black box) (C), WUS (red box) (D), and EUS (blue box) (E), respectively, for  
336 2000s (blue) and 2050s (red). Only grids over land in North America are used to generate  
337 the PDFs. The y-axis indicates the probability of occurrence of different PM<sub>2.5</sub> values shown  
338 in the x-axis. The colorbar illustrates PM<sub>2.5</sub> in ug/m<sup>3</sup>.

339

340 As anthropogenic- and wildfire-induced PM<sub>2.5</sub> concentrations may change differently  
341 with time across North America, next, we investigate the relative contribution of wildfire-  
342 induced PM<sub>2.5</sub> to the total PM<sub>2.5</sub> in the future. Prominent enhancement of the wildfire  
343 contribution is apparent in the entire domain by the 2050s (Figures 4A-B). Largely, during  
344 the 2000s, the simulated fractional contribution of wildfires to PM<sub>2.5</sub> is ~15-50 % in Canada  
345 (Figure 4A). Specifically, a bi-modal distribution is simulated over Canada with modal values  
346 around 18% and 30% (Figure 4C). Over WUS, the present day simulated percentage  
347 contributions of wildfire-induced values are 5-25% (Figure 4A), with modal values between  
348 10-20% (Figure 4D). Note that many areas located in the Pacific Northwest have higher  
349 values of ~30-40% (Figure 4A). At the same time, the fractional contribution by wildfire-  
350 induced PM<sub>2.5</sub> is ~5-10% in most areas of EUS in present day (Figure 4F). Nevertheless,  
351 some areas in the central US also have higher values of ~10-25% (Figure 4A).





353

354 **Figure 4: Spatial distribution and probability density function of the percentage**  
 355 **contribution of wildfire emissions.** A-B, Spatial distribution of the percentage contribution  
 356 of wildfire emissions to decadal-averaged summer (June through August; JJA) mean PM<sub>2.5</sub>  
 357 concentrations over North America during present day (A) and future (B). The percentage  
 358 contribution of wildfire-induced PM<sub>2.5</sub> to the total PM<sub>2.5</sub> concentrations is calculated as  
 359  $([2000_{ALL}-2000_{WEF}]/2000_{ALL})$  and  $([2050_{ALL}-2050_{WEF}]/2050_{ALL})$  for the present and future,  
 360 respectively. The grids with statistical significance of 90% is identified by black dots. C-E,  
 361 Probability density functions (PDFs) of the percentage wildfire contribution within the three  
 362 regions shown in Figure 2D for Canada (CND: black box) (C), WUS (red box) (D), and EUS  
 363 (blue box) (E), respectively, for the 2000s (blue) and the 2050s (red). Only grids over land in  
 364 North America are used to generate the PDFs. The y-axis indicates the probability of  
 365 occurrence of different PM<sub>2.5</sub> values shown in the x-axis.

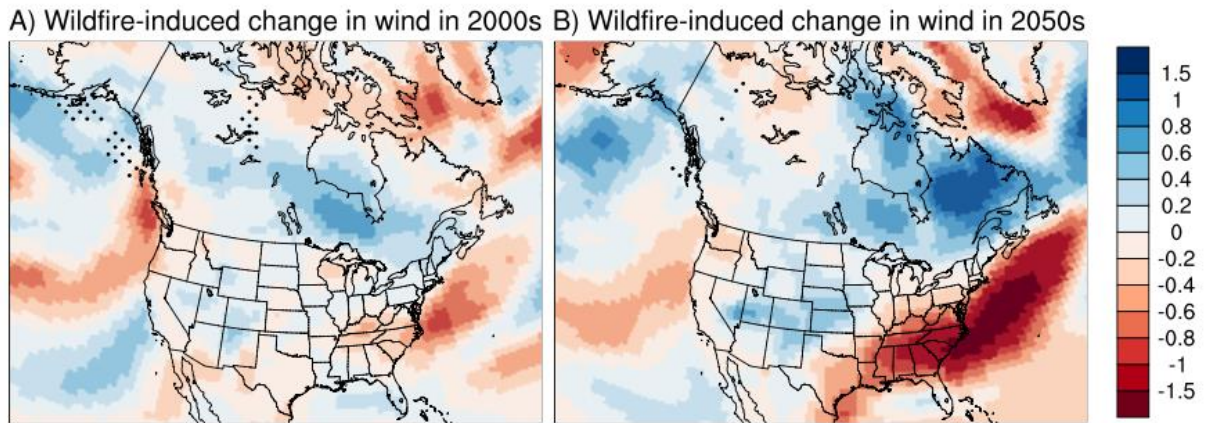
366

367 The wildfire contributions in the 2050s show a clear shift towards higher values in all  
 368 sub-regions compared to the 2000s (Figure 4B). Over Canada, the values shifted from 15-30  
 369 % in the 2000s to ~30-60% in the 2050s, a nearly two-fold increase in the fractional  
 370 contribution of wildfire emissions to the total PM<sub>2.5</sub> concentration is simulated (Figure 4B

371 and corresponding PDF in Figure 4C). Similarly, the contribution values increased to ~ 10-35  
372 % in the 2050s, compared to 10-20% in the 2000s over WUS (Figure 4B), thereby featuring a  
373 broadening of the bi-modal distribution of wildfire contribution (Figure 4D). The shift in the  
374 percentage contribution is most prominent for the higher values, corresponding to some areas  
375 located in the Pacific Northwest and west coast of the US (Figure 4B). Consistent with Figure  
376 3B, the shift in the contribution values over EUS is also very distinct, revealing an increase in  
377 the mode values from 6-10% in the 2000s to ~16-20 % by the 2050s (Figure 4B and Figure  
378 4E). Thus, not only in absolute values, but our results also underscore a large increase in the  
379 contribution of wildfire emissions over EUS in the future.

### 380 **3.3. Mechanistic understanding of the underlying processes**

381 The larger enhancement in the relative contribution of wildfire emissions to the total  
382 surface PM<sub>2.5</sub> in EUS in the 2050s can be explained by three mechanisms. First, due to the  
383 increase in Canadian and western US wildfires, downwind transport of wildfire smoke  
384 plumes to EUS will be enhanced by the 2050s. This long-range transport to the atmospheric  
385 column of EUS can happen within a few days of the fire occurrence (Supplementary Figures  
386 3A and 3B). Using Hazard Mapping System (HMS)-detected smoke plumes, recent studies  
387 identified a strong positive association between the transported smoke plumes in the  
388 atmospheric column and collocated surface PM<sub>2.5</sub> enhancement in EUS (Brey et al., 2018;  
389 Wu et al., 2018; Gunsch et al., 2018; Kaulfus et al., 2017; Larsen et al., 2017; Dempsey,  
390 2013). Hazard Mapping System (HMS) is an operational smoke detection product over North



391

392 **Figure 5a: Spatial distribution of decadal mean summer (June through August; JJA) wildfire-**  
 393 **induced future changes  $[(2050_{ALL}-2050_{WEF}) - (2000_{ALL}-2000_{WEF})]$ . A) Wind speed below 850**  
 394 **hpa for  $[(2050_{ALL}-2000_{ALL})]$ , B) Wind speed below 850 hpa  $[(2050_{WEF}) - (2000_{WEF})]$ . The**  
 395 **unit is m/s. The grids with statistical significance of 90% is identified by black dots.**

396 America known as developed by the National Oceanic and Atmospheric Administration  
 397 (NOAA) and operated by National Environmental Satellite, Data, and Information Service  
 398 (NESDIS), available at <http://satepsanone.nesdis.noaa.gov/FIRE/fire.html>. Specifically, these  
 399 studies found that the smoke plumes transported from Canada are located at an altitude of ~  
 400 1-3 km over EUS (Colarco et al., 2004; Wu et al., 2018). Due to mixing by the daytime  
 401 boundary layer and deposition, the smoke plumes enhance the surface PM<sub>2.5</sub> concentration  
 402 over EUS (Wu et al., 2018; Colarco et al., 2004; Rogers et al., 2020; Dreessen et al., 2015).  
 403 Hence HMS smoky days may be a useful proxy for wildfire-induced surface PM<sub>2.5</sub> over  
 404 North America. In agreement, Brey et al. (2018) showed that the HMS-based smoke plumes  
 405 observed over EUS is significantly aged, suggestive of their long-range transport origin.  
 406 Consistent with the observed temporal change in HMS pattern, Xue et al. (2021) estimated  
 407 using the mid-visible Multi Angle Implementation of Atmospheric Correction (MAIAC)  
 408 satellite-derived Aerosol Optical Depth (AOD) that Canadian and western US fires have  
 409 caused an increase in the daily PM<sub>2.5</sub> over Montana, North Dakota, South Dakota and  
 410 Minnesota by 18.3, 12.8, 10.4 and 10.1  $\mu g m^{-3}$ , respectively, between August 2011 (a low  
 411 fire month) and August 2018 (a high fire month). In summary, the visually apparent satellite-

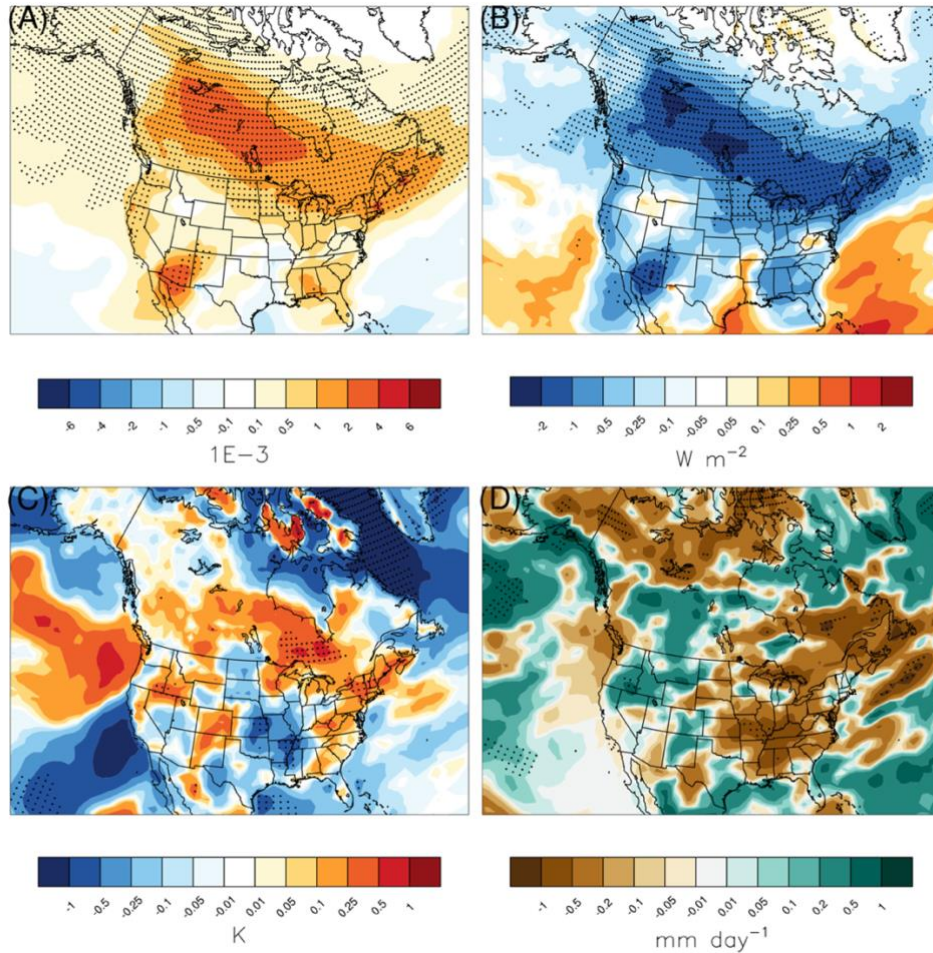
412 based signatures of wildfire-smoke across Canada and EUS provide a necessary, though not  
413 sufficient, support for the influence of Canadian smoke plumes on EUS air quality. Although,  
414 the change in burnt area over northeastern EUS is negligible compared to the western US and  
415 Canadian regions, however, there are some enhancements seen over east coast of US, which  
416 can also contribute to enhanced fire emissions.

417         In future, the wildfire-induced change in speed of the westerly jet flows over Canada  
418 wildfire regions is increased (Figure 5 A-B). It indicates that the transport of enhanced  
419 wildfire plumes from Canada boreal forests to the eastern half of Northern America and EUS  
420 will be enhanced in future compared to that in present era. On the one hand, the wildfire-  
421 induced changes in wind speed over the EUS is reduced in future, which implies that the  
422 local emissions over EUS are less dispersed. Simultaneously, this will also cause the  
423 transported smoke plumes to slow down and be subjected to relatively more boundary layer  
424 mixing over the EUS and dry deposition/settling enhances, thereby contributing to the  
425 enhanced PM<sub>2.5</sub> values at surface. The westerly winds over western US below 40° N is also  
426 strengthened in future (Figure 5 A-B) compared to present day which indicates more  
427 advection flux wildfire emissions to EUS. Thus, the net effect is enhanced removal of  
428 wildfire-emitted PM<sub>2.5</sub> from WUS and more influx of wildfire-emitted PM<sub>2.5</sub> in EUS.

429 Along with this dynamical changes, other climatic feedbacks simulated can also contribute to  
430 enhancement of EUS pollution. Specifically, the enhancement of wildfire-induced smoke  
431 aerosols increases solar absorption and scattering in the future (Figure 6A). This reduces the  
432 incoming solar radiation reaching at the surface (Figure 6B) and induces surface cooling.  
433 With atmospheric warming and surface cooling, lower-tropospheric stability is enhanced by  
434 wildfire aerosols in the future (Figure 6C). The smoke plumes which reaches eastern US are  
435 at an elevated altitude due to self-lofting property of absorbing aerosols as they travel

436 downwind but the smoke over western US is at near surface elevation as it is at its source  
437 region. This can explain the more significant atmospheric stability simulated over the eastern  
438 US compared to the source regions in western US and boreal forests of Canada. Relatively  
439 stronger atmospheric stability over eastern US impose a stronger thermal capping that traps  
440 more anthropogenic aerosols and particulate matter near the surface over EUS (already an  
441 emission hotspot). At the same time, future increase in wildfire emissions also leads to  
442 greater reduction of monthly rainfall (Figure 6D) over EUS, which may additionally  
443 strengthen the positive feedback to surface PM<sub>2.5</sub> over EUS by reducing wet scavenging of  
444 transported wildfire smoke to EUS. Thus, wildfire-emitted aerosols induce positive feedback  
445 on the surface PM<sub>2.5</sub> concentration over EUS through fire-climate interactions that vary on a  
446 regional scale. Moreover, the above discussed dynamical changes in future can also feedback  
447 these simulated thermodynamical and precipitation changes, exaggerating the enhancement in  
448 PM<sub>2.5</sub> values over EUS in future. However, due to computational constrains, no direct  
449 quantification of the magnitude of these feedback (with aerosol-radiation and aerosol-cloud  
450 interactions turned off) on PM<sub>2.5</sub> is performed and would be taken up in future studies.

451         Lastly, the reason of why the contribution of wildfire emissions to the total surface  
452 PM<sub>2.5</sub> in EUS is so substantial in the 2050s is the drastic reduction of anthropogenic  
453 contribution to the surface PM<sub>2.5</sub> over EUS in the future primarily due to policy-driven  
454 reduction in anthropogenic emissions under the RCP4.5 scenario. Specifically, the simulated  
455 ambient summer mean PM<sub>2.5</sub> concentration exhibits widespread declines in the future  
456 (Supplementary Figure 4), with reduction in PM<sub>2.5</sub> concentration over eastern US in the range  
457 of 4-15  $\mu\text{g}/\text{m}^3$ , which is greatest within North America. Thus, large reduction in  
458 anthropogenic contribution combined with increased downwind advection of Canadian  
459 smoke and WUS to EUS and the associated positive feedbacks can explain the projected  
460 dominance of wildfire emissions over EUS in future.



461

462 Figure 6: Spatial distribution of decadal mean summer (June through August; JJA) wildfire-  
 463 induced future changes  $[(2050_{ALL}-2050_{WEF}) - (2000_{ALL}-2000_{WEF})]$ . A) aerosol absorption  
 464 optical depth at 550 nm, B) aerosol direct radiative forcing at surface, C) lower-tropospheric  
 465 stability calculated as the difference between the potential temperature at 900 hPa and 1000  
 466 hPa, D) summer averaged precipitation rates, over North America. Areas marked with black  
 467 dots indicate grids where changes are significant at the 95% confidence level.

468

### 469 3.4 Future Implications and uncertainties

470

471

472

473

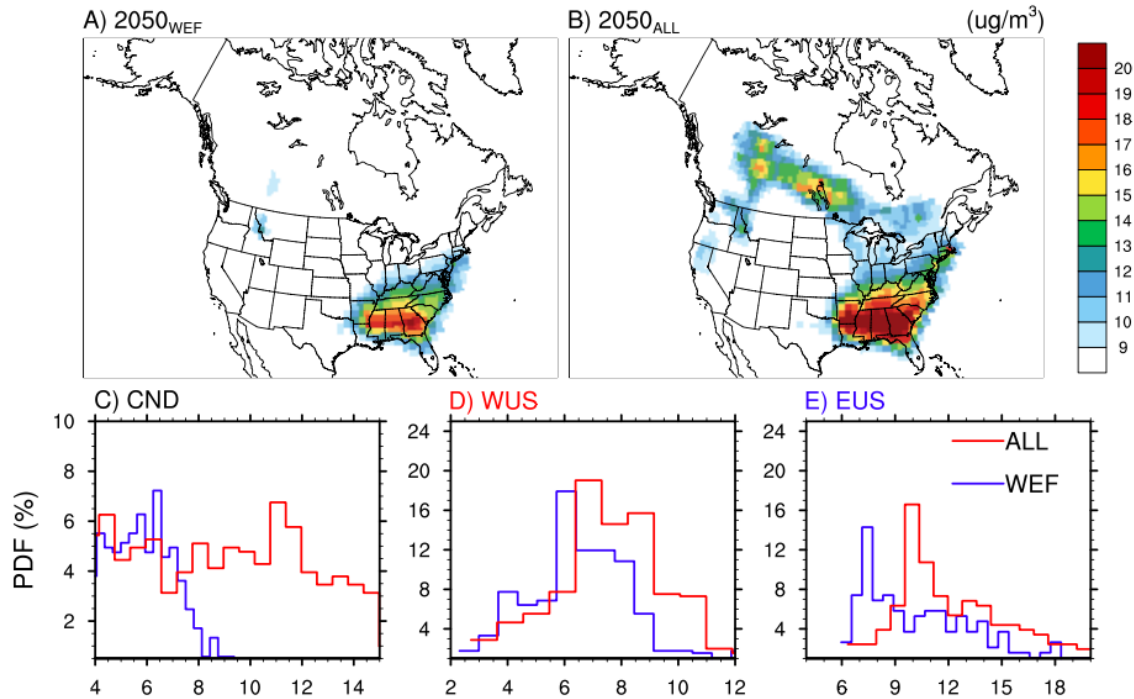
474

475

However, is the simulated future enhancement in wildfire contribution over EUS  
 substantial enough to affect the surface PM<sub>2.5</sub> values over EUS in future? The World Health  
 Organization (WHO) air quality guidelines for annual and daily PM<sub>2.5</sub> concentration are 10  
 $\mu\text{g m}^{-3}$  and 25  $\mu\text{g m}^{-3}$ , respectively. As no specific guideline for seasonal-mean PM<sub>2.5</sub> in the  
 summer is available, we use the annual guideline value as a reference to understand the  
 implication of wildfire emissions on ambient PM<sub>2.5</sub> concentration in the future. Interestingly,

476 the mean summertime PM<sub>2.5</sub> concentration in the wildfire emission free (WEF) scenario is  
477 projected to remain within 10 µg m<sup>-3</sup> over most of North America, except for the  
478 southeastern US (~15% of the domain) (Figure 7A). However, the ALL-scenario projects an  
479 increase in the exposure concentration level such that values > 10 µg/m<sup>3</sup> are common in  
480 Canada and EUS in the future (Figure 7B). Quantitatively, over Canada, the entire PDF of  
481 PM<sub>2.5</sub> concentration shifts towards higher values by ~5-6 µg/m<sup>3</sup>. Specifically, the modal value  
482 shifts from ~ 6 µg/m<sup>3</sup> in 2050<sub>WEF</sub> to 11-12 µg/m<sup>3</sup> in 2050<sub>ALL</sub> (Figure 7C), so PM<sub>2.5</sub>  
483 concentration is projected to surpass the WHO guidelines over a large fraction of Canada in  
484 the future. Similarly, the entire PDF of PM<sub>2.5</sub> concentration shifts towards higher values by  
485 ~2-3 µg/m<sup>3</sup> over EUS, with the mode of the PDF increasing from ~ 7-8 µg/m<sup>3</sup> in 2050<sub>WEF</sub> to  
486 ~ 10-11 µg/m<sup>3</sup> in 2050<sub>ALL</sub> (Figure 7E). The modal value of summer mean PM<sub>2.5</sub> over WUS  
487 increases from ~ 6 µg/m<sup>3</sup> in 2050<sub>WEF</sub> to ~ 7-8 µg/m<sup>3</sup> in 2050<sub>ALL</sub> (Figure 7D), although a few  
488 grid cells show PM<sub>2.5</sub> values greater than 10 µg/m<sup>3</sup> (Figure 7B).

489         Clearly, the climate-induced enhancement in fires and its influence via the advected  
490 wildfire smoke to EUS can have significant implications for air quality management in the  
491 future. The PM<sub>2.5</sub> enhancement in future over the southern states within EUS is large (Figure  
492 7A-B), which is consistent with Figure 3 and 4 results. However, the future change in burnt  
493 area over the same region is negligible or mostly reducing (Figure 1C-D). Thus, it can be  
494 argued that the simulated enhancement is mostly related with the dynamic perturbations and  
495 thermodynamical feedbacks due to wildfire emissions (Figure 6). As the rate of  
496 anthropogenic emissions is also regionally highest over the Southeastern states, the impact of  
497 these wildfire-induced climatic feedbacks on local air quality is distinctly seen over the EUS.



498

499 **Figure 7: Spatial distribution and probability density function of PM<sub>2.5</sub> concentration in**  
 500 **2050s. A-B**, Spatial distribution of decadal-average summer (June through August; JJA)  
 501 mean PM<sub>2.5</sub> concentration over North America in mid-21<sup>st</sup> century from 2050<sub>WEF</sub> (wildfire  
 502 emission-free) (A) and 2050<sub>ALL</sub> (wildfire emission-inclusive) (B). **C-E**, Probability density  
 503 functions (PDFs) of the same within the three regions shown in Figure 2B for Canada; CND  
 504 (C), western US; WUS (D), and eastern US; EUS (E), respectively, for the 2050<sub>WEF</sub> (blue)  
 505 and 2050<sub>ALL</sub> (red) runs. The y-axis indicates the probability of occurrence of different PM<sub>2.5</sub>  
 506 values shown in the x-axis. Only grids over land in North America are used to generate the  
 507 PDFs. Note the different ranges of values shown in the y- and x-axis in **C-E**. The colorbar  
 508 and the x-axis for Panel C-E indicates PM<sub>2.5</sub> values.

509 Note that our simulated present-day estimates of wildfire induced PM<sub>2.5</sub> values as well  
 510 as the percentage contribution of wildfire emissions are within the range of reported values in  
 511 previous studies over the domain, which augment the fidelity our future projections.  
 512 Specifically, our simulated present-day estimates of wildfire induced PM<sub>2.5</sub> values are also  
 513 within the range of reported values in previous studies over the domain. Reported values of  
 514 wildfire-induced PM<sub>2.5</sub> over WUS during summertime vary from  $\sim 1 \mu\text{g}/\text{m}^3$  (Jaffe et al., 2008)  
 515 to  $\sim 2 \mu\text{g}/\text{m}^3$  (Park et al., 2007) and  $\sim 3 \mu\text{g}/\text{m}^3$  (Ford et al., 2018), with the highest values  
 516 documented over the Pacific Northwest and west coast regions ( $\sim 1-4 \mu\text{g}/\text{m}^3$ ) (O'Dell et al.,  
 517 2019). The wildfire-induced PM<sub>2.5</sub> over EUS during summertime varies from  $\sim 1 \mu\text{g}/\text{m}^3$  (Park



518 et al., 2007) to  $\sim 2.5 \mu\text{g}/\text{m}^3$  ( $\sim 3 \mu\text{g}/\text{m}^3$  in the southeastern US) (Ford et al., 2018).  
519 Consistently, our simulated present-day estimates of wildfire contribution values are also  
520 within the range of reported values in previous studies. For example, Meng et al. (2019)  
521 found that wildfires can be the largest sectoral contributor ( $\sim 18\text{-}59\%$ ) to the population-  
522 weighted  $\text{PM}_{2.5}$  in various subregions of Canada. Over WUS, the present-day percentage  
523 contribution of wildfire induced  $\text{PM}_{2.5}$  to the total  $\text{PM}_{2.5}$  is reported to be  $\sim 12\%$  (Liu et al.,  
524 2017),  $\sim 15\%$  (Park et al., 2007) and  $\sim 30\%$  (Ford et al., 2018), with higher values of  $\sim 40\%$  in  
525 the Pacific Northwest (O'Dell et al., 2019). Over EUS our simulated values are also within  
526 the range of previously reported values of  $\sim 5\%$  (Park et al., 2007) and  $\sim 15\text{-}18\%$  (Ford et al.,  
527 2018). However, our two-way coupled simulations illustrate that future enhancement in the  
528 wildfire associated  $\text{PM}_{2.5}$  over the EUS could be greater compared to the western US, which  
529 is not emphasized explicitly in any of the previous studies (although Ford et al., 2018  
530 illustrated increase in  $\text{PM}_{2.5}$  over mid and central US from Canadian fires). These could be  
531 since inclusion of the wildfire-induced climatic feedbacks in our simulation is an  
532 unprecedented exercise. Please also note that our study is focused on JJA period and the  
533 wildfires in western US mainly occurs during August-September months, so the results  
534 should be compared consciously.

535         Nonetheless, inherent limitations in our simulations may introduce uncertainties in the  
536 projected future changes. For example, our reported changes in  $\text{PM}_{2.5}$  concentrations based on  
537 relatively coarse resolution simulations and decadal averages likely represent a low-end  
538 estimate compared to changes at regional and daily/weekly scales. Moreover, our  
539 experiments do not consider the direct human influences such as population change and  
540 socioeconomic development on wildfires, which may aggravate the increase in  $\text{PM}_{2.5}$   
541 concentrations over the densely populated EUS in the future. Common sources of uncertainty  
542 in modeling burnt area and fire emission and fire aerosol and smoke are also present in our

543 model. Fire smoke, in particular, is extremely hard to measure and evaluate. Lastly, inherent  
544 uncertainties in the physics parameterizations used in the model, sensitivity of climate to  
545 GHGs emissions, and the RCP scenarios should also be noted. Thus, ensemble modeling  
546 considering different emissions scenarios, population and future time periods, and the use of  
547 a finer spatial resolution may provide a more robust and better quantification of the wildfire-  
548 induced impact on policy regulated improvements in PM<sub>2.5</sub> over EUS.

#### 549 **4. Conclusion**

550 In summary, online coupled fire-climate-ecosystem simulations project a nearly  
551 twofold increase in wildfire-induced summer-mean surface PM<sub>2.5</sub> concentration by the mid-  
552 21<sup>st</sup> century over the entire North America. In a wildfire-emission free future, a large portion  
553 of North America will have PM<sub>2.5</sub> values below the WHO guidelines. But in a future with  
554 wildfire emissions, the improvements from policy-driven reductions in anthropogenic PM<sub>2.5</sub>  
555 will be compromised by the projected doubling of PM<sub>2.5</sub> from wildfires. More strikingly,  
556 wildfire-induced enhancement in surface PM<sub>2.5</sub> values and percentage contribution of the  
557 wildfire emissions over EUS could be substantial by mid-century. This is mainly because of  
558 the large enhancement in fires over Northern America by 2050s and associated increase in  
559 amount of downwind transport of smoke to EUS. In addition, enhancement of smoke  
560 transport induces a positive climate feedback to PM<sub>2.5</sub> concentrations over EUS by increasing  
561 the lower-tropospheric stability and reducing wet scavenging rates. Despite the inherent  
562 limitations, this study highlights the natural versus anthropogenic contributions and the non-  
563 local nature of air pollution that can complicate regulatory strategies aimed at improving air  
564 quality over the eastern US in a warmer future.

565

566

567 **Data availability statements**

568 The HMS data used in this paper are available free through the link  
569 <https://www.ospo.noaa.gov/Products/land/hms.html>. The model simulations data are  
570 available at <https://portal.nersc.gov/project/m1660/yang560/wildfire>

571 **Code availability statements**

572 The model code and scripts are available at  
573 <https://portal.nersc.gov/project/m1660/yang560/wildfire>

574

575 **Acknowledgements:**

576 This research was performed at PNNL and funded under Assistance Agreement No.  
577 RD835871 by the U.S. Environmental Protection Agency to Yale University through the  
578 SEARCH (Solutions for Energy, AiR, Climate, and Health) Center. It has not been formally  
579 reviewed by EPA. The views expressed in this document are solely those of the SEARCH  
580 Center and do not necessarily reflect those of the Agency. EPA does not endorse any  
581 products or commercial services mentioned in this publication. CS is supported by the New  
582 Faculty Initiation Grant project number CE/20-21/065/NFIG/008961 from IIT Madras.  
583 PNNL is operated by Battelle Memorial Institute for the U.S. Department of Energy under  
584 contract DE-AC06-76RLO-1830.

585

586 **Authors Contribution**

587 YQ, CS and RL designed this study. CS did the model and satellite analysis and wrote the  
588 first draft of the manuscript. YZou performed the simulations. All authors provided inputs  
589 throughout the study and helped in the drafting and submission process.

590

591 **References**

592 Abatzoglou, J. T. and Williams, A. P.: Impact of anthropogenic climate change on wildfire  
593 across western US forests, *Proc. Natl. Acad. Sci.*, 113(42), 11770 LP – 11775,  
594 doi:10.1073/pnas.1607171113, 2016.

595 Andela, N., Morton, D. C., Giglio, L., Chen, Y., van der Werf, G. R., Kasibhatla, P. S.,  
596 DeFries, R. S., Collatz, G. J., Hantson, S., Kloster, S., Bachelet, D., Forrest, M., Lasslop, G.,  
597 Li, F., Mangeon, S., Melton, J. R., Yue, C. and Randerson, J. T.: A human-driven decline in  
598 global burned area, *Science* (80-. ), 356(6345), 1356 LP – 1362,  
599 doi:10.1126/science.aal4108, 2017.

600 Anjali, H., Muhammad, A., Anthony, D. M., Karen, S., R., S. M., Mick, M., M., T. A., J., A.  
601 M. and Martine, D.: Impact of Fine Particulate Matter (PM<sub>2.5</sub>) Exposure During Wildfires on  
602 Cardiovascular Health Outcomes, *J. Am. Heart Assoc.*, 4(7), e001653,  
603 doi:10.1161/JAHA.114.001653, 2019.

604 Black, C., Tesfaigzi, Y., Bassein, J. A. and Miller, L. A.: Wildfire smoke exposure and  
605 human health: Significant gaps in research for a growing public health issue, *Environ.*

606 Toxicol. Pharmacol., 55, 186–195, doi:<https://doi.org/10.1016/j.etap.2017.08.022>, 2017.

607 Brey, S. J., Ruminski, M., Atwood, S. A. and Fischer, E. V: Connecting smoke plumes to  
608 sources using Hazard Mapping System (HMS) smoke and fire location data over North  
609 America, *Atmos. Chem. Phys.*, 18(3), 1745–1761, doi:10.5194/acp-18-1745-2018, 2018.

610 Dempsey, F.: Forest Fire Effects on Air Quality in Ontario: Evaluation of Several Recent  
611 Examples, *Bull. Am. Meteorol. Soc.*, 94(7), 1059–1064, doi:10.1175/BAMS-D-11-00202.1,  
612 2013.

613 Dominici, F., Peng, R. D., Bell, M. L., Pham, L., McDermott, A., Zeger, S. L. and Samet, J.  
614 M.: Fine Particulate Air Pollution and Hospital Admission for Cardiovascular and  
615 Respiratory Diseases, *JAMA*, 295(10), 1127–1134, doi:10.1001/jama.295.10.1127, 2006.

616 Diao, M., Holloway, T., Choi, S., O’Neill, S.M., Al-Hamdan, M.Z., Van Donkelaar, A.,  
617 Martin, R.V., Jin, X., Fiore, A.M., Henze, D.K. and Lacey, F., 2019. Methods, availability,  
618 and applications of PM<sub>2.5</sub> exposure estimates derived from ground measurements, satellite,  
619 and atmospheric models. *Journal of the Air & Waste Management Association*, 69(12),  
620 pp.1391-1414.

621 Ford, B., Val Martin, M., Zelasky, S. E., Fischer, E. V, Anenberg, S. C., Heald, C. L. and  
622 Pierce, J. R.: Future Fire Impacts on Smoke Concentrations, Visibility, and Health in the  
623 Contiguous United States, *GeoHealth*, 2(8), 229–247, doi:10.1029/2018GH000144, 2018.

624 Gillett, N. P., Weaver, A. J., Zwiers, F. W. and Flannigan, M. D.: Detecting the effect of  
625 climate change on Canadian forest fires, *Geophys. Res. Lett.*, 31(18),  
626 doi:10.1029/2004GL020876, 2004.

627 Gunsch, M. J., May, N. W., Wen, M., Bottenus, C. L. H., Gardner, D. J., VanReken, T. M.,  
628 Bertman, S. B., Hopke, P. K., Ault, A. P. and Pratt, K. A.: Ubiquitous influence of wildfire  
629 emissions and secondary organic aerosol on summertime atmospheric aerosol in the forested  
630 Great Lakes region, *Atmos. Chem. Phys.*, 18(5), 3701–3715, doi:10.5194/acp-18-3701-2018,  
631 2018.

632 Guan S, Wong DC, Gao Y, Zhang T, Pouliot G. Impact of wildfire on particulate matter in  
633 the southeastern United States in November 2016. *Sci Total Environ.* 2020;724:138354.  
634 doi:10.1016/j.scitotenv.2020.138354.

635 Johnston F. H., Henderson. S. B., Yang, C., T., R. J., Miriam, M., S., D. R., Patrick, K.,  
636 M.J.S., B. D. and Michael, B.: Estimated Global Mortality Attributable to Smoke from  
637 Landscape Fires, *Environ. Health Perspect.*, 120(5), 695–701, doi:10.1289/ehp.1104422,  
638 2012.

639 Harris, R. M. B., Remenyi, T. A., Williamson, G. J., Bindoff, N. L., and Bowman, D. M. J.  
640 S.: Climate-vegetation fire interactions and feedbacks: trivial detail or major barrier to  
641 projecting the future of the Earth system?, *Wires Clim. Change*, 7, 910-931,  
642 10.1002/wcc.428, 2016.

643 Hantson, S., Arneth, A., Harrison, S. P., Kelley, D. I., Prentice, I. C., Rabin, S. S., et al.  
644 (2016). The status and challenge of global fire modelling. *Biogeosciences*, 13, 3359–3375.  
645 <https://doi.org/10.5194/bg-13-3359-2016>

646 Hu, X., Yu, C., Tian, D., Ruminski, M., Robertson, K., Waller, L. A. and Liu, Y.:  
647 Comparison of the Hazard Mapping System (HMS) fire product to ground-based fire records

648 in Georgia, USA, *J. Geophys. Res. Atmos.*, 121(6), 2901–2910, doi:10.1002/2015JD024448,  
649 2016.

650 HURTT, G. C., FROLKING, S., FEARON, M. G., MOORE, B., SHEVLIAKOVA, E.,  
651 MALYSHEV, S., PACALA, S. W. and HOUGHTON, R. A.: The underpinnings of land-use  
652 history: three centuries of global gridded land-use transitions, wood-harvest activity, and  
653 resulting secondary lands, *Glob. Chang. Biol.*, 12(7), 1208–1229, doi:10.1111/j.1365-  
654 2486.2006.01150.x, 2006.

655 Jaffe, D., Hafner, W., Chand, D., Westerling, A. and Spracklen, D.: Interannual Variations in  
656 PM<sub>2.5</sub> due to Wildfires in the Western United States, *Environ. Sci. Technol.*, 42(8), 2812–  
657 2818, doi:10.1021/es702755v, 2008.

658 Jolly, W. M., Cochrane, M. A., Freeborn, P. H., Holden, Z. A., Brown, T. J., Williamson, G.  
659 J. and Bowman, D. M. J. S.: Climate-induced variations in global wildfire danger from 1979  
660 to 2013, *Nat. Commun.*, 6, 7537 [online] Available from:  
661 <https://doi.org/10.1038/ncomms8537>, 2015.

662 Kaulfus, A. S., Nair, U., Jaffe, D., Christopher, S. A. and Goodrick, S.: Biomass Burning  
663 Smoke Climatology of the United States: Implications for Particulate Matter Air Quality,  
664 *Environ. Sci. Technol.*, 51(20), 11731–11741, doi:10.1021/acs.est.7b03292, 2017.

665 Kirchmeier-Young, M. C., Zwiers, F. W., Gillett, N. P. and Cannon, A. J.: Attributing  
666 extreme fire risk in Western Canada to human emissions, *Clim. Change*, 144(2), 365–379,  
667 doi:10.1007/s10584-017-2030-0, 2017.

668 Kitzberger, T., Falk, D. A., Westerling, A. L. and Swetnam, T. W.: Direct and indirect  
669 climate controls predict heterogeneous early-mid 21st century wildfire burned area across  
670 western and North America, *PLoS One*, 12(12), e0188486 [online] Available from:  
671 <https://doi.org/10.1371/journal.pone.0188486>, 2017.

672 Knorr, W., Dentener, F., Lamarque, J.-F., Jiang, L. and Arneth, A.: Wildfire air pollution  
673 hazard during the 21st century, *Atmos. Chem. Phys.*, 17(14), 9223–9236, doi:10.5194/acp-  
674 17-9223-2017, 2017.

675 Koplitz, S.N., Nolte, C.G., Pouliot, G.A., Vukovich, J.M. and Beidler, J., 2018. Influence of  
676 uncertainties in burned area estimates on modeled wildland fire PM<sub>2.5</sub> and ozone pollution  
677 in the contiguous US. *Atmospheric environment*, 191, pp.328-339.

678 Lamarque, J. F., Bond, T. C., Eyring, V., Granier, C., Heil, A., Klimont, Z., Lee, D., Liousse,  
679 C., Mieville, A., Owen, 628 B., Schultz, M. G., Shindell, D., Smith, S. J., Stehfest, E., Van  
680 Aardenne, J., Cooper, O. R., Kainuma, M., 629 Mahowald, N., McConnell, J. R., Naik, V.,  
681 Riahi, K., and van Vuuren, D. P.: Historical (1850-2000) gridded anthropogenic and biomass  
682 burning emissions of reactive gases and aerosols: methodology and application, 631 *Atmos.*  
683 *Chem. Phys.*, 10, 7017-7039, 10.5194/acp-10-7017-2010, 2010.

684 Leibensperger, E. M., Mickley, L. J., Jacob, D. J., Chen, W.-T., Seinfeld, J. H., Nenes, A.,  
685 Adams, P. J., Streets, D. G., Kumar, N. and Rind, D.: Climatic effects of 1950–2050  
686 changes in US anthropogenic aerosols – Part 2: Climate response, *Atmos. Chem.*  
687 *Phys.*, 12(7), 3349–3362, doi:10.5194/acp-12-3349-2012, 2012.

688 Li, F., Zeng, X. D., & Levis, S. (2012). A process-based fire parameterization of intermediate  
689 complexity in a dynamic global vegetation model. *Biogeosciences*, 9(7), 2761–2780.  
690 <https://doi.org/10.5194/bg-9-2761-2012>

691 Liu, J. C., Mickley, L. J., Sulprizio, M. P., Dominici, F., Yue, X., Ebisu, K., Anderson, G. B.,  
692 Khan, R. F. A., Bravo, M. A. and Bell, M. L.: Particulate Air Pollution from Wildfires in the  
693 Western US under Climate Change, *Clim. Change*, 138(3), 655–666, doi:10.1007/s10584-  
694 016-1762-6, 2016.

695 Liu, Y., Goodrick, S. and Heilman, W.: Wildland fire emissions, carbon, and climate:  
696 Wildfire–climate interactions, *For. Ecol. Manage.*, 317, 80–96,  
697 doi:https://doi.org/10.1016/j.foreco.2013.02.020, 2014.

698 Liu, X., Easter, R. C., Ghan, S. J., Zaveri, R., Rasch, P., Shi, X., Lamarque, J. F., Gettelman,  
699 A., Morrison, H., Vitt, F., Conley, A., Park, S., Neale, R., Hannay, C., Ekman, A. M. L.,  
700 Hess, P., Mahowald, N., Collins, W., Iacono, M. J., Bretherton, C. S., Flanner, M. G., and  
701 Mitchell, D.: Toward a minimal representation of aerosols in climate models: description and  
702 evaluation in the Community Atmosphere Model CAM5, *Geosci. Model Dev.*, 5, 709- 652  
703 739, 10.5194/gmd-5-709-2012, 2012.

704 Meng, J., Martin, R.V., Li, C., van Donkelaar, A., Tzompa-Sosa, Z.A., Yue, X., Xu, J.W.,  
705 Weagle, C.L. and Burnett, R.T., 2019. Source Contributions to Ambient Fine Particulate  
706 Matter for Canada. *Environmental science & technology*, 53(17), pp.10269-10278.

707 McClure, C. D. and Jaffe, D. A.: US particulate matter air quality improves except in  
708 wildfire-prone areas, *Proc. Natl. Acad. Sci.*, 115(31), 7901 LP – 7906,  
709 doi:10.1073/pnas.1804353115, 2018.

710 Neale, R. B., Chen, C. C., Gettelman, A., Lauritzen, P. H., Park, S., Williamson, D. L.,  
711 Conley, A. J., Garcia, R., Kinnison, D., Lamarque, J. F., Marsh, D., Mills, M., Smith, A. K.,  
712 Tilmes, S., Vitt, F., Morrison, H., Cameron<sup>671</sup> Smith, P., Collins, W. D., Iacono, M. J.,  
713 Easter, R. C., Ghan, S. J., Liu, X. H., Rasch, P. J., and Taylor, M. A.: Description of the  
714 NCAR Community Atmosphere Model (CAM 5.0), NCAR 289, 2013

715 Nolte, C. G., Spero, T. L., Bowden, J. H., Mallard, M. S. and Dolwick, P. D.: The potential  
716 effects of climate change on air quality across the conterminous US at 2030 under three  
717 Representative Concentration Pathways, *Atmos. Chem. Phys.*, 18(20), 15471–15489,  
718 doi:10.5194/acp-18-15471-2018, 2018.

719 Katelyn O’Dell, Bonne Ford, Emily V. Fischer, and Jeffrey R. Pierce *Environmental Science*  
720 & *Technology* 2019 53 (4), 1797-1804, DOI: 10.1021/acs.est.8b05430.  
721

722 Partain, J. L., Alden, S., Strader, H., Bhatt, U. S., Bieniek, P. A., Brettschneider, B. R.,  
723 Walsh, J. E., Lader, R. T., Olsson, P. Q., Rupp, T. S., Thoman, R. L., York, A. D. and Ziel,  
724 R. H.: An Assessment of the Role of Anthropogenic Climate Change in the Alaska Fire  
725 Season of 2015, *Bull. Am. Meteorol. Soc.*, 97(12), S14–S18, doi:10.1175/BAMS-D-16-  
726 0149.1, 2016.

727 Park, S., Bretherton, C. S., and Rasch, P. J.: Integrating Cloud Processes in the Community  
728 Atmosphere Model, Version 5, *J. Climate*, 27, 6821-6856, 10.1175/Jcli-D-14-00087.1, 2014.

729 Park, R.J., Jacob, D.J. and Logan, J.A., 2007. Fire and biofuel contributions to annual mean  
730 aerosol mass concentrations in the United States. *Atmospheric Environment*, 41(35), pp.7389-  
731 7400.

732 Pierce, J. R., Val Martin, M., & Heald, C. L. (2017). Estimating the Effects of Changing  
733 Climate on Fires and Consequences for U.S. Air Quality, Using a Set of Global and Regional  
734 Climate Models (final report no. JFSP-13-1-01-4). Retrieved from

735 [https://www.firescience.gov/projects/13-1-01-4/project/13-1-01-4\\_final\\_report.pdf](https://www.firescience.gov/projects/13-1-01-4/project/13-1-01-4_final_report.pdf)

736 Pouliot G, Pace TG, Roy B, Pierce T, Mobley D. Development of a biomass burning  
737 emissions inventory by combining satellite and ground-based information. *J Appl Remote*  
738 *Sens.* 2008;2:021501. doi: 10.1117/1.2939551.

739 Randerson, J. T., Chen, Y., van der Werf, G. R., Rogers, B. M., & Morton, D. C. (2012).  
740 Global burned area and biomass burning emissions from small fires. *Journal of Geophysical*  
741 *Research*, 117, G04012. <https://doi.org/10.1029/2012JG002128>

742 Rolph, G. D., Draxler, R. R., Stein, A. F., Taylor, A., Ruminski, M. G., Kondragunta, S.,  
743 Zeng, J., Huang, H.-C., Manikin, G., McQueen, J. T. and Davidson, P. M.: Description and  
744 Verification of the NOAA Smoke Forecasting System: The 2007 Fire Season, *Weather*  
745 *Forecast.*, 24(2), 361–378, doi:10.1175/2008WAF2222165.1, 2009.

746 Spracklen, D. V., Mickley, L. J., Logan, J. A., Hudman, R. C., Yevich, R., Flannigan, M. D.,  
747 & Westerling, A. L. (2009). Impacts of climate change from 2000 to 2050 on wildfire activity  
748 and carbonaceous aerosol concentrations in the western United States. *Journal of Geophysical*  
749 *Research*, 114, D20301. <https://doi.org/10.1029/2008JD010966>

750 Sun, Y., Gu, L. H., and Dickinson, R. E.: A numerical issue in calculating the coupled carbon  
751 and water fluxes in a climate model, *J. Geophys. Res.-Atmos.*, 117,  
752 D2210310.1029/2012jd018059, 2012

753 Sofiev, M., Ermakova, T., and Vankevich, R.: Evaluation of the smoke-injection height from  
754 wild-land fires using remote-sensing data, *Atmos. Chem. Phys.*, 12, 1995-2006, 10.5194/acp-  
755 12-1995-2012, 2012

756 Shi, H., Jiang, Z., Zhao, B., Li, Z., Chen, Y., Gu, Y., Jiang, J. H., Lee, M., Liou, K.-N., Neu,  
757 J. L., Payne, V. H., Su, H., Wang, Y., Witek, M. and Worden, J.: Modeling Study of the Air  
758 Quality Impact of Record-Breaking Southern California Wildfires in December 2017, *J.*  
759 *Geophys. Res. Atmos.*, 0(0), doi:10.1029/2019JD030472, 2019.

760 U.S. EPA (U.S. Environmental Protection Agency). 2009. Integrated Science Assessment  
761 (ISA) For Particulate Matter (Final Report). EPA/600/R-08/139F. Washington, DC:U.S. EPA.

762 U.S. EPA. 2018. Our Nation's Air. <https://gispub.epa.gov/air/trendsreport/2018/>

763 Val Martin, M., Heald, C. L., Lamarque, J.-F., Tilmes, S., Emmons, L. K. and Schichtel, B.  
764 A.: How emissions, climate, and land use change will impact mid-century air quality over the  
765 United States: a focus on effects at national parks, *Atmos. Chem. Phys.*, 15(5), 2805–2823,  
766 doi:10.5194/acp-15-2805-2015, 2015.

767 Van der Werf, G. R., Randerson, J. T., Giglio, L., Collatz, G. J., Kasibhatla, P. S., and  
768 Arellano, A. F.: Interannual variability in global biomass burning emissions from 1997 to  
769 2004, *Atmos. Chem. Phys.*, 6, 3423-3441, DOI 737 10.5194/acp-6-3423-2006, 2006

770 Van Der Werf, G. R., Randerson, J. T., Giglio, L., Collatz, G. J., Mu, M., Kasibhatla, P. S.,  
771 Morton, D. C., Defries, R. S., Jin, Y. and Van Leeuwen, T. T.: Global fire emissions and the  
772 contribution of deforestation, savanna, forest, agricultural, and peat fires (1997-2009), *Atmos.*  
773 *Chem. Phys.*, 10(23), 11707–11735, doi:10.5194/acp-10-11707-2010, 2010.

774 Van Donkelaar, A., R. V. Martin, M. Brauer, N. C. Hsu, R. A. Kahn, R. C. Levy, A.  
775 Lyapustin, A. M. Sayer, and D. M. Winker. 2018. Global Annual PM<sub>2.5</sub> Grids from MODIS,  
776 MISR and SeaWiFS Aerosol Optical Depth (AOD) with GWR, 1998-2016. Palisades NY:

777 NASA Socioeconomic Data and Applications Center (SEDAC).  
778 <https://doi.org/10.7927/H4ZK5DQS>. Accessed 16 November 2019.

779 Ward, D. S., Kloster, S., Mahowald, N. M., Rogers, B. M., Randerson, J. T. and Hess, P. G.:  
780 The changing radiative forcing of fires: global model estimates for past, present and future,  
781 *Atmos. Chem. Phys.*, 12(22), 10857–10886, doi:10.5194/acp-12-10857-2012, 2012.

782 Wotton, B. M., Flannigan, M. D., and Marshall, G. A.: Potential climate change impacts on  
783 fire intensity and key wildfire suppression thresholds in Canada, *Environ. Res. Lett.*, 12,  
784 095003, <https://doi.org/10.1088/1748-9326/aa7e6e>, 2017.

785 Westerling, A. L., Hidalgo, H. G., Cayan, D. R. and Swetnam, T. W.: Warming and Earlier  
786 Spring Increase Western U.S. Forest Wildfire Activity, *Science* (80-. ), 313(5789), 940 LP –  
787 943, doi:10.1126/science.1128834, 2006.

788 Wotawa, G. and Trainer, M.: The Influence of Canadian Forest Fires on Pollutant  
789 Concentrations in the United States, *Science* (80-. ), 288(5464), 324 LP – 328,  
790 doi:10.1126/science.288.5464.324, 2000.

791 Wu, Y., Arapi, A., Huang, J., Gross, B. and Moshary, F.: Intra-continental wildfire smoke  
792 transport and impact on local air quality observed by ground-based and satellite remote  
793 sensing in New York City, *Atmos. Environ.*, 187, 266–281,  
794 doi:<https://doi.org/10.1016/j.atmosenv.2018.06.006>, 2018.

795 Xue, Z., Gupta, P., and Christopher, S.: Satellite-based estimation of the impacts of  
796 summertime wildfires on PM<sub>2.5</sub> concentration in the United States, *Atmos. Chem. Phys.*, 21,  
797 11243–11256, <https://doi.org/10.5194/acp-21-11243-2021>, 2021.

798 Yang, P.-L., Y. Zhang, K. Wang, P. Doraiswamy, and S.-H. Cho, 2019, Health Impacts and  
799 Cost-Benefit Analyses of Surface O<sub>3</sub> and PM<sub>2.5</sub> over the U.S. under Future Climate and  
800 Emission Scenarios, *Environmental Research*, 178, November 2019, 108687,  
801 <https://doi.org/10.1016/j.envres.2019.108687>.

802 Yue, X., Mickley, L. J., Logan, J. A. and Kaplan, J. O.: Ensemble projections of wildfire  
803 activity and carbonaceous aerosol concentrations over the western United States in the mid-  
804 21st century, *Atmos. Environ.*, 77, 767–780,  
805 doi:<https://doi.org/10.1016/j.atmosenv.2013.06.003>, 2013.

806 Zou, Y., Wang, Y., Ke, Z., Tian, H., Yang, J. and Liu, Y.: Development of a REgion-Specific  
807 Ecosystem Feedback Fire (RESFire) Model in the Community Earth System Model, *J. Adv.  
808 Model. Earth Syst.*, 11(2), 417–445, doi:10.1029/2018MS001368, 2019.

809 Zou, Y., Wang, Y., Qian, Y., Tian, H., Yang, J. and Alvarado, E.: Using CESM-RESFire to  
810 understand climate–fire–ecosystem interactions and the implications for decadal climate  
811 variability, *Atmos. Chem. Phys.*, 20, 995–1020, <https://doi.org/10.5194/acp-20-995-2020>,  
812 2020.

813 Zhang, Y., P.-L. Yang, Y. Gao, R. L. Leung, and M. Bell, 2020, Health and Economic  
814 Impacts of Air Pollution Induced by Climate Extremes over the Continental U.S.,  
815 *Environmental International*, 143, 105921, <https://doi.org/10.1016/j.envint.2020.105921>.

816

817